RAA 2016 Vol. **16** No. **9**, 142 (8pp) doi: 10.1088/1674–4527/16/9/142
http://www.raa-journal.org *http://iopscience.iop.org/raa*

Research in Astronomy and Astrophysics

The use of laser altimetry data in Chang'E-1 precision orbit determination

Sheng-Qi Chang[1,2], Yong Huang[1], Pei-Jia Li[1], Xiao-Gong Hu[1] and Min Fan[1,2,3]

[1] Key Laboratory of Planetary Sciences, Shanghai Astronomical Observatory, Chinese Academy of Sciences, Shanghai 200030, China; *changsq@shao.ac.cn*
[2] University of Chinese Academy of Sciences, Beijing 100049, China
[3] Beijing Institute of Tracking and Telecommunications Technology, Beijing 100094, China

Received 2016 April 3; accepted 2016 May 12

Abstract Accurate altimetric measurement not only can be applied to the calculation of a topography model but also can be used to improve the quality of the orbit reconstruction in the form of crossovers. Altimetry data from the Chang'E-1 (CE-1) laser altimeter are analyzed in this paper. The differences between the crossover constraint equation in the form of height discrepancies and in the form of minimum distances are mainly discussed. The results demonstrate that the crossover constraint equation in the form of minimum distances improves the CE-1 orbit precision. The overlap orbit performance has increased $\sim 30\%$ compared to the orbit using only tracking data. External assessment using the topography model also shows orbit improvement. The results will be helpful for recomputing ephemeris and improving the CE-1 topography model.

Key words: celestial mechanics — methods: data analysis — Moon

1 INTRODUCTION

The laser altimetric instrument is one of the most important payloads on a lunar explorer. A laser altimeter was first carried on Apollo 15 to measure the Moon in 1971 (Kaula et al. 1972), and since then, laser altimetry has been the primary tool used to measure the size and shape of the Moon in lunar and deep space explorations. In recent years, a series of lunar explorers, including China's Chang'E-1 (CE-1; Ping et al. 2009) and Chang'E-2 (CE-2; Li et al. 2012), JAXA's SELenological and ENgineering Explorer (SELENE; Kato et al. 2008), NASA's Lunar Reconnaissance Orbiter (LRO; Chin et al. 2007; Smith et al. 2010), and India's Chandrayaan-1 (Kamalakar et al. 2005), all carried laser altimetry equipment (Table 1).

Laser altimetry data can be used not only in the calculation of a topography model but also in the precision orbit determination (POD) of spacecraft, as has been performed for ocean altimetry satellites, such as TOPEX/ERS-1 and Jason-1 (Shum et al. 1990; Luthcke et al. 2003). In deep space exploration, Rowlands et al. (1999) used altimetric crossovers for the orbit reconstruction of the Mars Global Surveyor (MGS) probe and the instrument pointing offset estimation of the Mars Orbiter Laser Altimeter (MOLA). Additionally, incorporating MOLA altimeter crossover data into the calculation of the Mars gravity field improved the quality of the gravity field model (Lemoine et al. 2001). Lunar Orbiter Laser Altimeter (LOLA) was a 10-cm-precision 28-Hz, five-beam laser altimeter mounted on Lunar Reconnaissance Orbiter (LRO). Because of LOLA's high precision and spatial resolution, significant improvements were obtained by using altimetric crossovers in the orbit determination process (Rowlands et al. 2009; Mazarico et al. 2012). Goossens et al. (2011) indicated that improvements only occurred in certain situations with the inclusion of altimetric crossovers on SELENE, which was mainly caused by the poor spatial resolution of the Laser ALTtimeter (LALT). Vighnesam et al. (2009) used altimetric data directly with the topography model rather than using crossover constraints.

Yan et al. (2010) evaluated the orbit precision of CE-1 between 2007 November 20 and 29, with Unified S-Band (USB) ranging data and Very Long Baseline Interferometry (VLBI) data. The radial error of overlap was approximately 15–30 m, which was limited by the tracking data coverage. The LAM, laser altimetry instrument on CE-1, began to work on November 28, and the ranging accuracy was approximately 5 m in the aircraft tests (Ping et al. 2009). LAM measurements could be obtained from both the far side and the near side of the Moon, thereby significantly increasing the useful observational coverage. In this paper, we take altimetric crossovers into orbit determination to improve the orbit precision of CE-1. Crossover analysis of LAM data has been tested by Hu et al. (2013) (using a non-dynamical method different from the one described in this paper) and has been shown to improve the topography model.

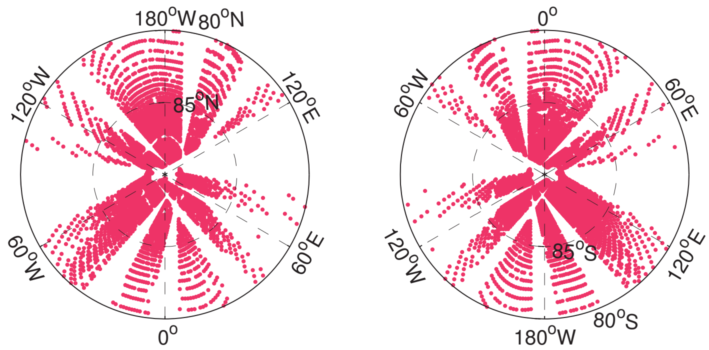

Fig. 1 Plot of crossover distribution for 2007.11.27–2007.12.25 (*left*: Latitude $> 80^\circ$; *right*: Latitude $< -80^\circ$).

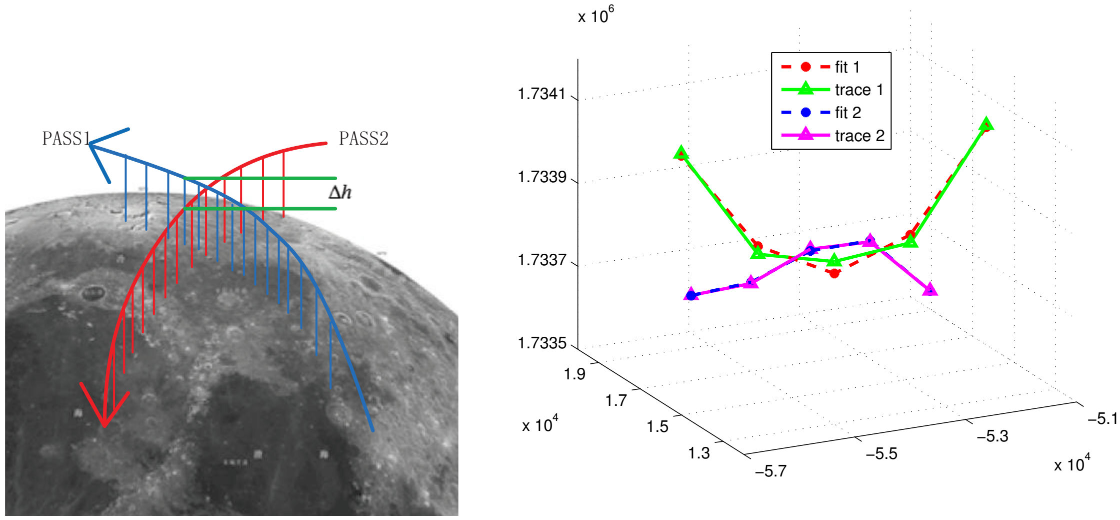

Fig. 2 Diagram of height discrepancy crossover (*left*) and diagram of minimum distance crossover (*right*).

Table 1 Specifications of Altimetry Instrument on CE-1/SELENE/LRO/Chandrayaan

	CE-1	SELENE	LRO	Chandrayaan-1
Orbit altitude (km)	200	100	50	100
Distance error (m)	5	4.1	<1	5
Sampling rate (Hz)	1	1	28	10
Radial orbit error (m)	15	1	1	/
3D orbit error (m)	$\sim$200	$\sim$50	$\sim$20	$\sim$150
Footprint (m)	$< \phi 200$	/ 40	5 / beam	100

2 CROSSOVER CONSTRAINT EQUATION

At each intersection between two altimetry tracks, called a crossover, the same topography should be measured. Two crossing passes provide independent measurements at the same location at different times. Altimetry data can provide constraints on the orbit in the form of crossovers. Because the CE-1 probe has a polar circular orbit with an inclination angle of 88.2° and the Moon rotates very slowly, the tracks of sub-satellite points are basically parallel with the longitude in low latitude so that most crossovers are located near the pole. In this study, ground tracks of the probe are fit with discrete Legendre polynomials to obtain a better accuracy of crossover locations. Furthermore, due to the slow rotation of the Moon, the time interval between the intersections of ascending and descending tracks is at least one week. To achieve a reasonably full coverage of crossovers, we select the altimetric data with a span of 28 days to calculate crossovers (Fig. 1). Therefore the state of multiple arcs of CE-1 probe must to be estimated simultaneously, which will be explained specifically in the next section.

Shum et al. (1990) gave a detailed description of the use of crossovers in orbit determination and gravity field

Table 2 Numbers of Tracking Data and Crossovers in Each Batch

	Start epoch	Duration days	Number (Range)	Number (VLBI delay)	Number (VLBI delay rate)	Number (Crossovers)
Batch 1	2007-11-27	30	576162	62270	58863	27898
Batch 2	2007-12-27	28	347653	75076	100158	29074
Batch 3	2008-01-09	29	301224	71508	101559	24150
Batch 4	2008-05-14	28	302937	91750	81756	22198
Batch 5	2008-06-08	29	292274	84399	63261	29599

Table 3 Some Parameters Used in the Orbit Determination

Item	Model
N-body perturbation	Sun, major planets, Earth and Moon, DE421 ephemeris
Solar radiation pressure	Fixed area-mass ratio (prior $C_r = 1.24$)
Non-spherical gravitational perturbation	Lunar gravity field model GRAIL660, degree and order truncated to 165
Estimated Parameters	Position, velocity, solar radiation pressure, range bias, empirical constant acceleration in radial-transverse-normal (RTN) direction
Data and weight	Range: 3 m Delay: 3 ns Delay rate: 0.3 ps s^{-1} Crossover: 20 m

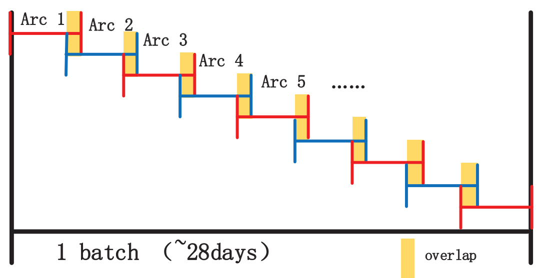

Fig. 3 Diagram of arc distribution in a batch.

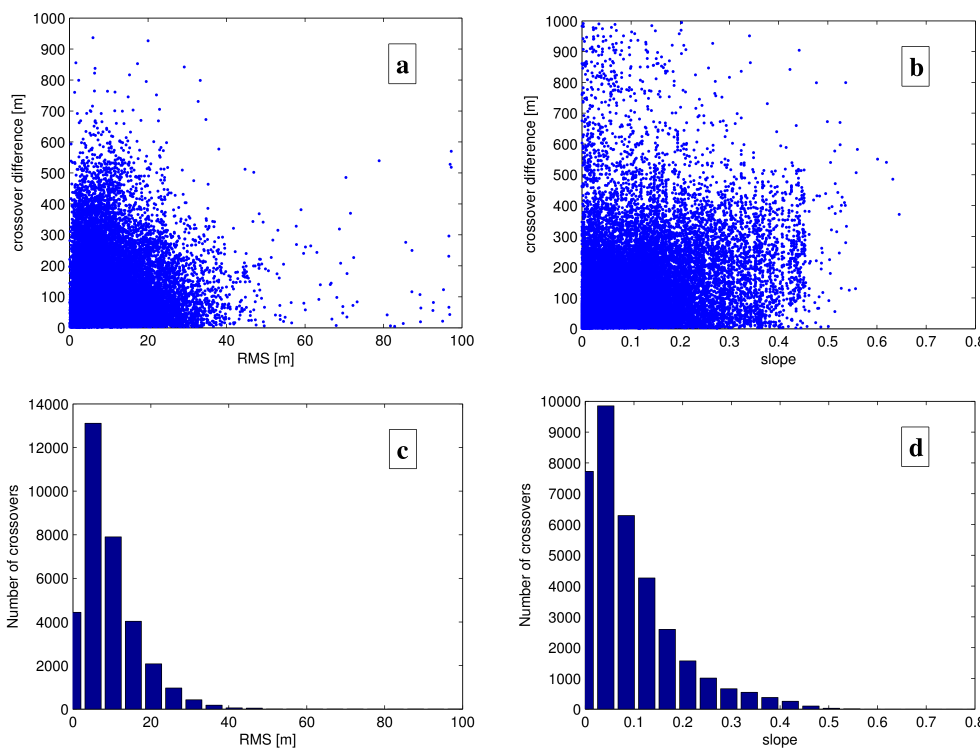

Fig. 4 Plot of crossover differences versus (a) RMS of polynomial fit and (b) slope; histogram displaying the number of crossovers versus (c) RMS of polynomial fit and (d) slope.

estimation for the case of radar (large footprint) altimetry over deep oceans. The crossover constraint equation in the form of height discrepancies is given as

$$O - C = [\mathrm{alt}(t_i) - \mathrm{alt}(t_j)] - [h(t_i) - h(t_j)], \qquad (1)$$

where t_i and t_j are the times when ground tracks of ascending and descending arcs intersect, respectively and $\mathrm{alt}(t_i)$ and $h(t_i)$ are the altimetric measurement and the altitude of the satellite at t_i, respectively (Fig. 2 (left)). This type of crossover constraint equation is sensitive to the radial component of an orbit. Precision improvement was only found in the radial direction when this form of crossover was used in Jason-1's POD (Luthcke et al. 2003).

To increase the sensitivity to the horizontal orbit error, Rowlands et al. (1999) put forward a crossover constraint equation formulated in the form of minimum distance. In the vicinity of the location where a conventional crossover (height discrepancy) occurs, the X, Y and Z planet-fixed coordinates of the bounce points of the laser beams on the lunar surface of each pass can separately be fit with a polynomial in time (Fig. 2 (right)). Then, we use these six polynomials to determine the two planet-fixed location points and also the times (t_i and t_j) at which two passes come closest. The minimum distance between two curves (i.e., the distance between these two points) represents the crossover discrepancy. In this study, a cubic polynomial fit by five points is adopted. For this type of crossover, the observed value is set to be zero, so the residual is the negative of the minimum distance. The crossover constraint equation is defined as follows

$$O - C \;=\; \Delta d(t_i, t_j) = |\boldsymbol{x_b}'(t_i) - \boldsymbol{x_b}'(t_j)|, \qquad (2)$$

$$\boldsymbol{x_b}'(t_i) \;=\; \boldsymbol{x_b}(t_i) - \mathrm{alt}(t_i)\cdot\frac{\boldsymbol{x_b}(t_i)}{|\boldsymbol{x_b}(t_i)|}, \qquad (3)$$

where $\boldsymbol{x_b}(t_i)$ is the position vector of the satellite in the planet-fixed coordinate. This form of crossover constraint equation enables sensitivity to directions other than the radial one. In the next section, we will describe how these two types of crossover constraints interact in an orbit determination.

3 DATA AND ORBIT DETERMINATION STRATEGY

All calculations in this article were performed using software developed at the Shanghai Astronomical Observatory (SHAO), Chinese Academy of Sciences (Huang et al. 2014). USB range data from Qingdao and Kashi and VLBI data from Shanghai, Beijing, Kunming and Urumqi are used in POD. Level 2 altimetric data provided by the Science and Application Center for Moon and Deepspace Exploration[1] include level 2A products and level 2B products. The level 2A data are a series of original altimetric measurements after bias and pointing corrections are applied and the level 2B data are the product when level 2A data are geolocated. In orbit adjustment, level 2A data are included to compute crossovers.

We process the orbit from 2007 November 26 to 2008 July 8, as we do not have angular momentum desaturation (AMD) information after 2008 July 8, which is essential to POD. In addition, LAM took a 3-month-long break after 2008 February 7. This means that approximately five months' worth of altimetric data are available. The batch statistics are shown in Table 2.

The arc length of CE-1 is set to be $36 \sim 48\,\mathrm{h}$ which is long enough to include tracking data from Qingdao and Kashi, but short enough to avoid modeling-related errors and the overlap of two consecutive arcs is set to be $2 \sim 4\,\mathrm{h}$ (Fig. 3). To obtain full coverage of crossovers, a span of approximately 28 days of altimetric data is selected to calculate crossovers so that we can divide all of these data into five batches. Orbit determination is an iterative procedure, so for each iteration of the batch, we re-determine the crossovers when the estimate of the orbit evolves. This means that the states of approximately $14'' \sim 16''$ need to be estimated simultaneously.

In the CE-1 mission, the spacecraft attitude was controlled using AMD. In this study, AMD events are considered in the orbit determination process, by estimating empirical accelerations or delta-velocities during the event (Huang et al. 2009). Data weights used in the processing are shown in Table 3. Ground tracking data weights are at the same level as their actual data fit value after orbit adjustment. However, the RMS value of crossover discrepancies is higher than the data weight of 20 m (see Table 4). This data weight is chosen to emphasize the crossover in orbit determination because there are far fewer crossovers than ground tracking data.

In the calculation of crossover discrepancies, the interpolation of crossover locations and corresponding heights or distances introduces several uncertainties. To avoid introducing more errors into the crossover discrepancies, we should eliminate crossovers that are not suitable for orbit determination. Rowlands et al. (1999) and Neumann et al. (2001) used very strict edit criteria when they analyzed data from MOLA: the polynomials fit should be better than 5 m and the point-to-point slope should be smaller than 0.1. MOLA's high sampling rate (10 Hz) allowed the researchers to be this strict. LAM's sampling rate, however, is 1 Hz, the same as LALT, so we adopt looser edit criteria, similar to those used by Goossens et al. (2011).

In Figure 4(a) and (b), crossover discrepancies (minimum distance between two curves) are not increasing when the RMS of polynomial fit or slopes become larger, which means even high RMS of fit or large slopes can still have small crossover discrepancies.

Figure 4(c) and (d) show that crossovers with polynomial fits better than 40 m are up to 98% and slopes smaller than 0.2 are approximately 86%. In this study, data with a fit worse than 40 m and slope larger than 0.2 were deleted. Furthermore, crossover differences larger than 500 m are excluded in the orbit processing.

[1] *http://moon.bao.ac.cn/ceweb/datasrv/dmsce1.jsp*

Table 4 RMS of Data Fit Statistics of POD in Strategy C

	Batch 1	Batch 2	Batch 3	Batch 4	Batch 5
Range (m)	3.9	3.5	3.3	2.7	2.9
VLBI delay (ns)	5.37	4.2	3.7	7.8	5.9
VLBI delay rate (ps s^{-1})	0.90	0.57	0.57	1.33	0.83
Crossovers (m)	100.7	99.3	93.7	82.4	80.8

Table 5 RMS of Orbit Overlap Differences for CE-1 in the Local Satellite Orbit Frame

Batch	Data Combination	Radial [m]	Along [m]	Cross [m]	Total [m]
1	A	8.43	178.65	117.25	220.39
	B	24.50	205.26	124.85	252.88
	C	8.56	161.23	71.17	182.34
2	A	11.64	70.83	50.82	104.41
	B	14.72	86.06	52.81	120.93
	C	9.59	63.13	42.53	85.95
3	A	5.91	31.53	31.11	51.95
	B	9.68	49.87	30.58	69.77
	C	7.27	28.15	12.00	34.23
4	A	8.66	118.23	119.22	183.42
	B	8.97	117.61	126.01	189.53
	C	9.59	111.23	84.31	151.43
5	A	13.38	111.95	109.18	172.25
	B	17.64	106.42	101.64	160.44
	C	12.54	51.50	42.61	74.05

Notes– Data combination A: USB+VLBI, B: USB+VLBI+1st crossover and C: USB+VLBI+2nd crossover.

4 RESULTS AND ANALYSIS

To evaluate the influence of adding crossovers in orbit adjustment, three strategies are considered in the POD analysis: (a) ground tracking data only; (b) addition of altimetric crossovers in the form of height discrepancy; (c) addition of altimetric crossovers in the form of minimum distance.

The data fit is quite stable from batch to batch. It is necessary to note that the change in data fit of ground tracking data is very tiny after adding crossovers in orbit adjustment.

In Table 4, crossovers are in the form of minimum distance, and as for strategy B, RMS of crossovers in the form of height difference is between 73 m and 104 m. Although LAM and LALT share the same level of sampling rate and ranging precision (Ping et al. 2009; Araki et al. 1999), crossover discrepancies of LALT after orbit adjustment were 24 m (Goossens et al. 2011), much smaller than LAM. The average altitude of SELENE was 100 km, while that of CE-1 was 200 km, so the diameter of LALT's footprint was much smaller than that of LAM. A larger footprint introduces more error when altimetric data are geolocated. Moreover, the radial precision of SELENE is approximately 1 m, which is much better than that of CE-1. It is understandable that crossover discrepancies are at a level of 90 m.

We assess the orbit precision by evaluating the RMS position difference of the trajectories computed in consecutive arc pairs during their overlapping period.

In Figure 5, tracking data of arcs in purple rectangles include ranging measurements and VLBI measurements. Otherwise, only ranging data are included. Obviously, VLBI data contribute a lot to orbit precision when only ground tracking data are used in POD. In batch 2 and batch 3, most arcs contain VLBI measurements; therefore, the orbit precision of these two batches performs better than the other three batches. Orbit errors in some arcs are extremely large (> 500 m); these are mainly caused by orbit maneuvers.

The addition of crossovers in the form of height discrepancy does not make any progress in orbit adjustment; some batches perform even worse than the results in which only ground tracking data are used. As the error of the prior orbit (i.e., the orbit only using ground tracking data) is mainly in the along-track and cross-track directions, height discrepancies caused by horizontal orbit error will be aliased into the radial component. Crossover constraints written as height discrepancies cannot improve the horizontal orbit error.

Compared to the result from only ground tracking data, adding crossovers in the form of minimum distance significantly improves the orbit consistency, and the overall overlap RMS in total position decreases from ~ 147 m to ~ 105 m (average of strategy A and strategy C of the last column in Table 5), a 30% reduction. After each iteration in adjustment, the locations of crossovers change not only because of the change of the orbit solution; the distance minimization process moves them as well. Crossovers tie separate arcs of the satellite together and this helps especially when one of the orbits is not well determined from the tracking data alone so that the orbit error is more homogeneous.

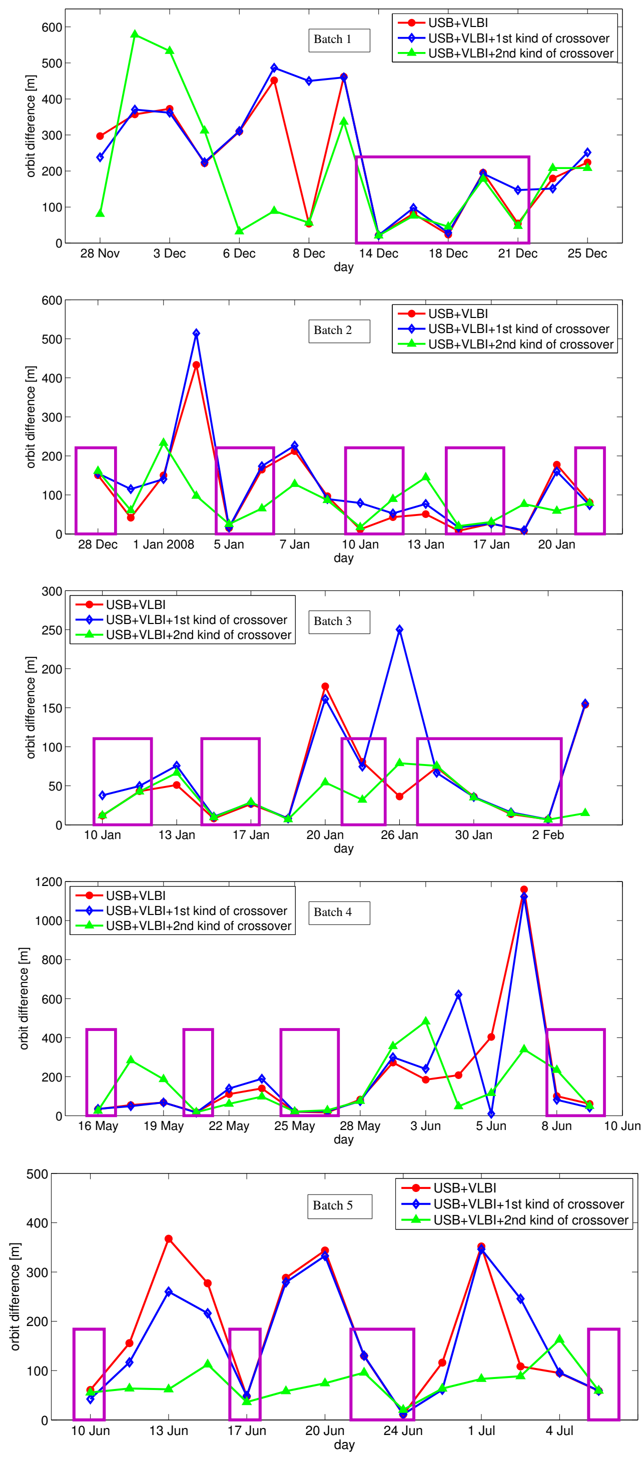

Fig. 5 Plot of RMS of total orbit overlap differences for each batch.

In Figure 5, we can hardly find notable outliers of orbit differences after using this type of crossover constraint in adjustment. The contributions of crossover constraint under the conditions with and without VLBI measurements are also analyzed. Orbit precision improves from 189 m to 136 m after adding crossovers in orbit adjustment when VLBI measurements are unavailable. As for the conditions with VLBI measurements, orbit precision has barely changed (from 51 m to 52 m) after adding crossovers. So, crossover constraint provides a complement to those arcs without VLBI tracking.

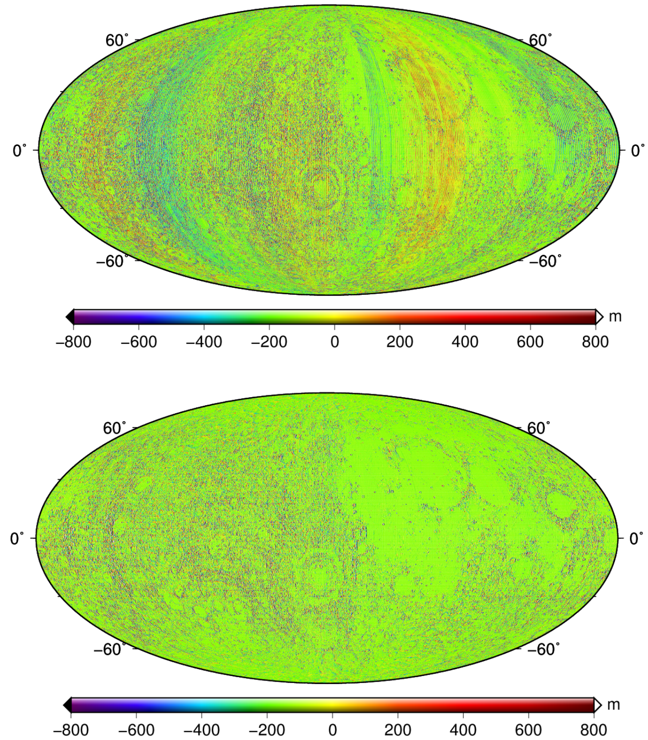

Fig. 6 Differences of topography model compared to LOLA: model from LAM 2B level product (*upper*); model from altimetric data geolocated with the orbit result in this article (*bottom*).

Because of the limited coverage of ground tracking, especially for VLBI, the orbit precision of CE-1 is poorer than LRO ($\sim$ 24 m) and SELENE ($\sim$ 50 m) when only using radiometric data. Additional crossovers in POD help LRO achieve position accuracy of approximately 13 m, a 50% reduction (Mazarico et al. 2012). As for SELENE, crossover constraints also improve the orbit when the coverage of crossovers is relatively full (Goossens et al. 2011).

Furthermore, we assess the orbit result externally. First, we use the LAM 2B level product to calculate a lunar topography model. Then, the orbit results in this article are applied to geolocate the LAM 2A level product so that another topography model can be created. Both of the topography models are compared to the topography model derived from LOLA altimetric data (Smith et al. 2011). The RMS of elevation differences between the CE-1 topography model and LOLA topography model decreases from 350 m to 219 m after applying the new orbit results in the CE-1 topography model. The maximum and minimum elevation differences also improve from 20.0 km and -20.9 km to 11.7 km and -13.5 km, respectively. In Figure 6 (left), striped differences can be seen clearly; these are mainly caused by the orbit error. With the new orbit results, a better topography model is obtained, and no more significant striped differences can be found.

5 CONCLUSIONS

In this paper, we present the application of laser altimetric data from LAM to orbit adjustment. Crossover constraints written as height discrepancies could not contribute to orbit consistency in the CE-1 orbit process. Combining crossovers in the form of minimum distances improves orbit quality. Compared to the orbit using only tracking data, overall overlap RMS in total position decreases from $\sim$ 147 m to $\sim$ 105 m. We adopt external assessment of the orbit as well. Comparison of topography models confirms the improvement on POD. This result will be helpful in improving the CE-1 topography model.

Acknowledgements This work was supported by the National Natural Science Foundation of China (11473056 and 11403076) and the Science and Technology Commission of Shanghai (3912DZ227330001).

References

Araki, H., Ooe, M., Tsubokawa, T., et al. 1999, Advances in Space Research, 23, 1813

Chin, G., Brylow, S., Foote, M., et al. 2007, Space Sci. Rev., 129, 391

Goossens, S., Matsumoto, K., Rowlands, D. D., et al. 2011, Journal of Geodesy, 85, 487

Hu, W., Di, K., Liu, Z., & Ping, J. 2013, Planet. Space Sci., 87, 173

Huang, Y., Hu, X., Huang, C., Yang, Q., & Jiao, W. 2009, Science in China: Physics, Mechanics and Astronomy, 52, 346

Huang, Y., Chang, S., Li, P., et al. 2014, Chinese Science Bulletin, 59, 3858

Kamalakar, J. A., Bhaskar, K. V. S., Laxmi Prasad, A. S., et al. 2005, Journal of Earth System Science, 114, 725

Kato, M., Sasaki, S., Tanaka, K., Iijima, Y., & Takizawa, Y. 2008, Advances in Space Research, 42, 294

Kaula, W. M., Schubert, G., Lingenfelter, R. E., Sjogren, W. L., & Wollenhaupt, W. R. 1972, in Lunar and Planetary Science Conference Proceedings, 3, eds. A. E. Metzger, J. I. Trombka, L. E. Peterson, R. C. Reedy, & J. R. Arnold, 2189 (*http://issfd.org/ISSFD_2009/OrbitDeterminationII/Vighnesam2.pdf*)

Lemoine, F. G., Smith, D. E., Rowlands, D. D., et al. 2001, J. Geophys. Res., 106, 23359

Li, P., Hu, X., Huang, Y., et al. 2012, Science China Physics, Mechanics, and Astronomy, 55, 514

Luthcke, S., Zelensky, N., Rowlands, D., Lemoine, F., & Williams, T. 2003, Marine Geodesy, 26, 399

Mazarico, E., Rowlands, D. D., Neumann, G. A., et al. 2012, Journal of Geodesy, 86, 193

Neumann, G. A., Rowlands, D. D., Lemoine, F. G., Smith, D. E., & Zuber, M. T. 2001, J. Geophys. Res., 106, 23753

Ping, J., Huang, Q., Yan, J., et al. 2009, Science in China Series G: Physics, Mechanics and Astronomy, 52, 1105

Rowlands, D. D., Lemoine, F. G., Chinn, D. S., & Luthcke, S. B. 2009, Journal of Geodesy, 83, 709

Rowlands, D. D., Pavlis, D. E., Lemoine, F. G., Neumann, G. A., & Luthcke, S. B. 1999, Geophys. Res. Lett., 26, 1191

Shum, C. K., Schutz, B. E., Tapley, B. D., & Zhang, B. H. 1990, Journal of the Astronautical Sciences, 38, 355

Smith, D. E., Zuber, M. T., Jackson, G. B., et al. 2010, Space Sci. Rev., 150, 209

Smith, D. E., Zuber, M. T., Neumann, G. A., et al. 2011, in Lunar and Planetary Science Conference, 42, 2350

Vighnesam, N.V., Anatta sonney, & Gopinath N.S. 2009, 21st ISSFD, Toulouse: ISSFD, 51

Yan, J., Ping, J., Li, F., et al. 2010, Advances in Space Research, 46, 50